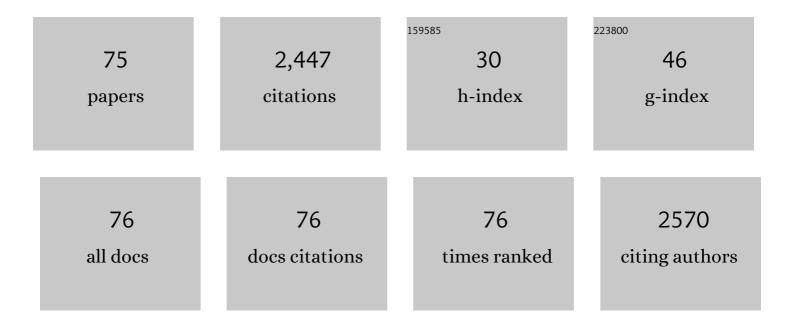
List of Publications by Year in descending order

Source: https://exaly.com/author-pdf/2025852/publications.pdf Version: 2024-02-01



MINC SHEN

#	Article	IF	CITATIONS
1	High Anodic Performance of Co 1,3,5-Benzenetricarboxylate Coordination Polymers for Li-Ion Battery. ACS Applied Materials & Interfaces, 2016, 8, 15352-15360.	8.0	181
2	A new insight into the lithium storage mechanism of sulfurized polyacrylonitrile with no soluble intermediates. Energy Storage Materials, 2018, 14, 272-278.	18.0	140
3	Ultrathin Manganese-Based Metal–Organic Framework Nanosheets: Low-Cost and Energy-Dense Lithium Storage Anodes with the Coexistence of Metal and Ligand Redox Activities. ACS Applied Materials & Interfaces, 2017, 9, 29829-29838.	8.0	131
4	The organic-moiety-dominated Li ⁺ intercalation/deintercalation mechanism of a cobalt-based metal–organic framework. Journal of Materials Chemistry A, 2016, 4, 16245-16251.	10.3	116
5	A thermally activated manganese 1,4-benzenedicarboxylate metal organic framework with high anodic capability for Li-ion batteries. New Journal of Chemistry, 2016, 40, 9746-9752.	2.8	104
6	Superionic Conductors <i>via</i> Bulk Interfacial Conduction. Journal of the American Chemical Society, 2020, 142, 18035-18041.	13.7	101
7	Facile synthesis of the Basolite F300-like nanoscale Fe-BTC framework and its lithium storage properties. RSC Advances, 2016, 6, 114483-114490.	3.6	79
8	Solitons shedding from Airy beams and bound states of breathing Airy solitons in nonlocal nonlinear media. Scientific Reports, 2015, 5, 9814.	3.3	76
9	Unraveling the Critical Role of Ti Substitution in P ₂ -Na _{<i>x</i>} Li _{<i>y</i>} Mn _{1–<i>y</i>} O ₂ Cathodes for Highly Reversible Oxygen Redox Chemistry. Chemistry of Materials, 2020, 32, 1054-1063.	6.7	74
10	Carbon-coated Li3V2(PO4)3 derived from metal-organic framework as cathode for lithium-ion batteries with high stability. Electrochimica Acta, 2018, 271, 608-616.	5.2	52
11	Simple Transformation of Covalent Organic Frameworks to Highly Proton-Conductive Electrolytes. ACS Applied Materials & Interfaces, 2020, 12, 8198-8205.	8.0	51
12	Interactions of nonlocal dark solitons under competing cubic–quintic nonlinearities. Optics Letters, 2014, 39, 1764.	3.3	50
13	Reversible lithium storage in manganese and cobalt 1,2,4,5-benzenetetracarboxylate metal–organic framework with high capacity. RSC Advances, 2016, 6, 61319-61324.	3.6	45
14	Capacity control of ferric coordination polymers by zinc nitrate for lithium-ion batteries. RSC Advances, 2016, 6, 86126-86130.	3.6	42
15	Exploring the Capacity Limit: A Layered Hexacarboxylate-Based Metal–Organic Framework for Advanced Lithium Storage. Inorganic Chemistry, 2018, 57, 3126-3132.	4.0	41
16	Control on the anomalous interactions of Airy beams in nematic liquid crystals. Optics Express, 2016, 24, 8501.	3.4	39
17	High-energy nanostructured Na ₃ V ₂ (PO ₄) ₂ O _{1.6} F _{1.4} cathodes for sodium-ion batteries and a new insight into their redox chemistry. Journal of Materials Chemistry A. 2018. 6. 8340-8348.	10.3	39
18	A rings-in-pores net: crown ether-based covalent organic frameworks for phase-transfer catalysis. Chemical Communications, 2020, 56, 595-598.	4.1	39

#	Article	IF	CITATIONS
19	Nonlocal incoherent white-light solitons in logarithmically nonlinear media. Physical Review E, 2005, 72, 026604.	2.1	38
20	Broadband finite-pulse radio-frequency-driven recoupling (fp-RFDR) with (XY8)41 super-cycling for homo-nuclear correlations in very high magnetic fields at fast and ultra-fast MAS frequencies. Journal of Magnetic Resonance, 2012, 223, 107-119.	2.1	37
21	Anionic redox reactions and structural degradation in a cation-disordered rock-salt Li _{1.2} Ti _{0.4} Mn _{0.4} O ₂ cathode material revealed by solid-state NMR and EPR. Journal of Materials Chemistry A, 2020, 8, 16515-16526.	10.3	37
22	Tunable lateral shift and polarization beam splitting of the transmitted light beam through electro-optic crystals. Journal of Applied Physics, 2008, 104, .	2.5	35
23	Stabilization of vortex solitons by combining competing cubic-quintic nonlinearities with a finite degree of nonlocality. Physical Review A, 2014, 89, .	2.5	35
24	The electrochemical Na intercalation/extraction mechanism of ultrathin cobalt(II) terephthalate-based MOF nanosheets revealed by synchrotron X-ray absorption spectroscopy. Energy Storage Materials, 2018, 14, 82-89.	18.0	35
25	Unraveling the Redox Couples of V ^{III} /V ^{IV} Mixed-Valent Na ₃ V ₂ (PO ₄) ₂ O _{1.6} F _{1.4} Cathode by Parallel-Mode EPR and In Situ/Ex Situ NMR. Journal of Physical Chemistry C, 2018, 122, 27224-27232.	3.1	35
26	Instability suppression of clusters of vector-necklace-ring solitons in nonlocal media. Physical Review A, 2011, 83, .	2.5	33
27	Dark solitons in nonlocal media with competing nonlinearities. Physical Review A, 2013, 87, .	2.5	32
28	Polymer chain diffusion and Li + hopping of poly(ethylene oxide)/LiAsF 6 crystalline polymer electrolytes as studied by solid state NMR and ac impedance. Solid State Ionics, 2014, 255, 74-79.	2.7	31
29	Host–Guest Interactions in Dealuminated HY Zeolite Probed by ¹³ C– ²⁷ Al Solid-State NMR Spectroscopy. Journal of Physical Chemistry Letters, 2014, 5, 3068-3072.	4.6	31
30	Room-temperature synthesis of a cobalt 2,3,5,6-tetrafluoroterephthalic coordination polymer with enhanced capacity and cycling stability for lithium batteries. New Journal of Chemistry, 2017, 41, 1813-1819.	2.8	31
31	Highly reversible lithium storage in cobalt 2,5-dioxido-1,4-benzenedicarboxylate metal-organic frameworks boosted by pseudocapacitance. Journal of Colloid and Interface Science, 2017, 506, 365-372.	9.4	31
32	Deciphering the Origin of High Electrochemical Performance in a Novel Ti-Substituted P2/O3 Biphasic Cathode for Sodium-Ion Batteries. ACS Applied Materials & Interfaces, 2020, 12, 41485-41494.	8.0	31
33	Partially coherent accessible solitons in strongly nonlocal media. Physical Review E, 2006, 73, 056602.	2.1	29
34	High-capacity cobalt-based coordination polymer nanorods and their redox chemistry triggered by delocalization of electron spins. Energy Storage Materials, 2017, 7, 195-202.	18.0	28
35	Guided modes near the Dirac point in negative-zero-positive index metamaterial waveguide. Optics Express, 2010, 18, 12779.	3.4	26
36	Solid-state NMR indirect detection of nuclei experiencing large anisotropic interactions using spinning sideband-selective pulses. Solid State Nuclear Magnetic Resonance, 2015, 72, 104-117.	2.3	25

#	Article	IF	CITATIONS
37	Alâ€doped SBAâ€15 Catalysts for Lowâ€ŧemperature Dehydration of 1,3â€Butanediol into Butadiene. ChemCatChem, 2017, 9, 258-262.	3.7	25
38	A facile route for preparing a mesoporous palladium coordination polymer as a recyclable heterogeneous catalyst. Dalton Transactions, 2012, 41, 4692.	3.3	23
39	Stability of optical solitons in parity-time-symmetric optical lattices with competing cubic and quintic nonlinearities. Physical Review E, 2015, 91, 023203.	2.1	23
40	Monitoring the evolution of local oxygen environments during LiCoO ₂ charging <i>via ex situ</i> ¹⁷ 0 NMR. Chemical Communications, 2019, 55, 7550-7553.	4.1	21
41	Melatonin Represses Mitophagy to Protect Mouse Granulosa Cells from Oxidative Damage. Biomolecules, 2021, 11, 968.	4.0	21
42	Tunable band gap near the Dirac point in nonlinear negative-zero-positive index metamaterial waveguide. Physical Review A, 2011, 83, .	2.5	20
43	Improving the resolution in proton-detected through-space heteronuclear multiple quantum correlation NMR spectroscopy. Journal of Magnetic Resonance, 2014, 245, 38-49.	2.1	20
44	Operando EPR and EPR Imaging Study on a NaCrO ₂ Cathode: Electronic Property and Structural Degradation with Cr Dissolution. Journal of Physical Chemistry Letters, 2021, 12, 781-786.	4.6	19
45	Comparison of various NMR methods for the indirect detection of nitrogen-14 nuclei via protons in solids. Journal of Magnetic Resonance, 2015, 258, 86-95.	2.1	18
46	Tailoring Anionic Redox Activity in a P2-Type Sodium Layered Oxide Cathode via Cu Substitution. ACS Applied Materials & Interfaces, 2022, 14, 28738-28747.	8.0	18
47	A multifunctional manipulation to stabilize oxygen redox and phase transition in 4.6 V high-voltage LiCoO2 with sXAS and EPR studies. Journal of Power Sources, 2021, 516, 230661.	7.8	17
48	Dipole solitons in nonlocal nonlinear media with anisotropy. Optics Communications, 2011, 284, 2351-2356.	2.1	16
49	Probing Local Structure of Layered Double Hydroxides with ¹ H Solid-State NMR Spectroscopy on Deuterated Samples. Journal of Physical Chemistry Letters, 2014, 5, 363-369.	4.6	16
50	Mesoporous cobalt 2,5-thiophenedicarboxylic coordination polymer for high performance Na-ion batteries. Materials Letters, 2017, 197, 245-248.	2.6	15
51	Reversible High-Voltage N-Redox Chemistry in Metal–Organic Frameworks for High-Rate Anion-Intercalation Batteries. ACS Applied Energy Materials, 2019, 2, 413-419.	5.1	14
52	Melatonin Alleviates Hypoxia-Induced Apoptosis of Granulosa Cells by Reducing ROS and Activating MTNR1B–PKA–Caspase8/9 Pathway. Antioxidants, 2021, 10, 184.	5.1	14
53	Incoherent accessible white-light solitons in strongly nonlocal Kerr media. Physical Review E, 2006, 74, 027601.	2.1	13
54	Suppression of collapse for two-dimensional Airy beam in nonlocal nonlinear media. Scientific Reports, 2017, 7, 4198.	3.3	12

#	Article	IF	CITATIONS
55	Incoherent interactions of Airy beams in nonlocal nonlinear media. Journal of Physics B: Atomic, Molecular and Optical Physics, 2018, 51, 165401.	1.5	12
56	Broad-band excitation in indirectly detected 14 N overtone spectroscopy with composite pulses. Solid State Nuclear Magnetic Resonance, 2016, 78, 5-8.	2.3	11
57	The interaction of dark solitons with competing nonlocal cubic nonlinearities. Journal of Optics (India), 2015, 44, 271-280.	1.7	10
58	ECNU-10 zeolite: A three-dimensional MWW-Type analogue. Microporous and Mesoporous Materials, 2017, 253, 137-145.	4.4	10
59	Effect of Exogenous Melatonin on the Development of Mice Ovarian Follicles and Follicular Angiogenesis. International Journal of Molecular Sciences, 2021, 22, 11262.	4.1	10
60	Revisiting NMR composite pulses for broadband 2 H excitation. Solid State Nuclear Magnetic Resonance, 2015, 66-67, 45-48.	2.3	9
61	High-fidelity spectroscopy reconstruction in accelerated NMR. Chemical Communications, 2018, 54, 10958-10961.	4.1	9
62	Elliptic fundamental, dipole and vortex solitons in nonlocal nonlinear media with linear anisotropic diffraction. Journal of Optics (United Kingdom), 2020, 22, 025502.	2.2	9
63	The phase structure, chain diffusion motion and local reorientation motion: 13C Solid-state NMR study on the highly-crystalline solid polymer electrolytes. Polymer, 2014, 55, 5454-5459.	3.8	8
64	Observation of 1H–13C and 1H–1H proximities in a paramagnetic solid by NMR at high magnetic field under ultra-fast MAS. Journal of Magnetic Resonance, 2015, 251, 36-42.	2.1	8
65	Retarding Phase Transformation During Cycling in a Lithium―and Manganeseâ€Rich Cathode Material by Optimizing Synthesis Conditions. ChemElectroChem, 2019, 6, 1385-1392.	3.4	8
66	The dependence of signal-to-noise ratio on number of scans in covariance spectroscopy. Solid State Nuclear Magnetic Resonance, 2014, 59-60, 31-33.	2.3	7
67	Collapse arrest in a two-dimensional Airy Gaussian beam and Airy Gaussian vortex beam in nonlocal nonlinear media. Communications in Theoretical Physics, 2022, 74, 025501.	2.5	7
68	Reduction of the 13C cross-polarization experimental time for pharmaceutical samples with long T1 by ball milling in solid-state NMR. Solid State Nuclear Magnetic Resonance, 2018, 94, 20-25.	2.3	6
69	Exploring various modulation-sideband recoupling conditions of SHA+ sequence at fast MAS. Solid State Nuclear Magnetic Resonance, 2013, 55-56, 42-47.	2.3	5
70	Tunneling modes and giant Goos–Hächen effect of a symmetric heterostructure containing negative-zero-positive index metamaterials. Applied Physics B: Lasers and Optics, 2015, 120, 69-73.	2.2	5
71	The study of electrochemical cycle for LiCoO2 by dual-mode EPR. Magnetic Resonance Letters, 2023, 3, 61-66.	1.3	4
72	Elimination of the baseline distortions in WURST-CPMG static experiments. Solid State Nuclear Magnetic Resonance, 2016, 78, 1-4.	2.3	2

#	Article	IF	CITATIONS
73	Goos-Hiichen shifts for a one-dimensional photonic crystal with a nonlinear defect. , 2006, , .		Ο
74	The analyses of negative refraction in finite one-dimensional photonic crystals. , 2006, , .		0
75	Guided modes of surface plasmon polaritons in linear dielectric–metal–nonlinear dielectric waveguide. Optik, 2018, 174, 216-220.	2.9	0